Contents lists available at ScienceDirect

Journal of King Saud University – Science

journal homepage: www.sciencedirect.com

Carbon nanotubes-based nanohybrids for multifunctional nanocomposites

Rossella Arrigo [a,b,*], Sonia Bellavia [a], Cristian Gambarotti [c], Nadka Tzankova Dintcheva [a], Sabrina Carroccio [d]

[a] Dipartimento di Ingegneria Civile, Ambientale, Aerospaziale, dei Materiali, Università degli Studi di Palermo, Viale delle Scienze, Ed. 6, 90128 Palermo, Italy
[b] Dipartimento di Scienza Applicata e Tecnologia, Politecnico di Torino, Viale Teresa Michel 5, 15121 Alessandria, Italy
[c] Dipartimento di Chimica, Materiali ed Ingegneria Chimica "G. Natta", Politecnico di Milano, Piazza L. da Vinci 32, 20133 Milano, Italy
[d] Consiglio Nazionale delle Ricerche – IMM s.s Catania (Università), Via S. Sofia 64, 95123 Catania, Italy

ARTICLE INFO

ABSTRACT

In the present work, nano-hybrids based on carbon nanotubes (CNTs) bearing immobilized, either through covalent linkage and physical absorption, commercial anti-oxidant molecules have been formulated and used as nanofillers in Ultra High Molecular Weight Polyethylene (UHMWPE), aiming at preparing multifunctional nanocomposites. The effective immobilization of the anti-oxidant molecules has been probed by spectroscopic and thermogravimetric analyses. The study of the morphology and the rheological behaviour of the nanocomposites show that the immobilization of anti-oxidant molecules onto the CNTs surface is beneficial for the state of the polymer/nanoparticles interfacial region. Additionally, the study of the nanocomposites thermo-oxidative behaviour reveals that the nano-hybrids are able to exert a remarkable anti-oxidant action which is related to the strong interactions established between the anti-oxidant molecules and the CNTs, resulting in the formation of structural defects onto the CNTs surface and in the consequent amplification of the intrinsic CNTs radical scavenging activity.

1. Introduction

Recently, significant efforts have been directed toward the formulation of multi-functional polymer-based nanocomposites containing hybrid nanoparticles (Arrigo et al., 2016a; Jie et al., 2015). In particular, carbon nanotubes (CNTs) have received a great attention as nanofillers for polymer-based complex systems, due to their unique combination of mechanical, electrical and magnetic properties (Coleman et al., 2006; Spitalsky et al., 2010). Furthermore, the CNTs surface can be easily modified with several functional groups carrying specific functionalities through different strategies, such as defect (Mawhinney et al., 2000) and covalent

(Yang et al., 2007) functionalization. Interestingly, a promising strategy to modify the CNTs surface without compromise their structural integrity involves the non-covalent functionalization of CNTs with molecules showing a strong affinity with graphitic surfaces of CNTs (Nativ-Roth et al., 2007; Chen et al., 2008). An interesting paper by Pan et al. (Pan and Xing, 2008) reports the different mechanisms of adsorption of organic molecules on CNTs; in the case of aromatic moieties, the physical adsorption is believed to be due to the π-π electron coupling (Lin and Xing, 2008, Wang et al., 2010) between adsorbate molecules and carbon nanotube surfaces and this hypothesis is corroborated by experimental study and density functional theory calculations (Mallakpour and Soltanian, 2016). Moreover, recent studies (Yu et al., 2016) show that the π–π interactions between aromatic compounds and graphitic surfaces increased with increasing aromatic rings in aromatic molecules.

The modification of the CNTs surface, besides provide them with new functionalities, helps to enhance the state of the polymer/CNTs interfacial region, bringing about the obtainment of nanocomposites with superior properties, suitable for advanced applications (Arrigo et al., 2016b).

Recent researches have shown that CNTs are able to exert an excellent anti-oxidant action against the thermo- and

* Corresponding author at: Dipartimento di Ingegneria Civile, Ambientale, Aerospaziale, dei Materiali, Università degli Studi di Palermo, Viale delle Scienze, Ed. 6, 90128 Palermo, Italy.

E-mail address: rossella.arrigo@polito.it (R. Arrigo).

Production and hosting by Elsevier

photo-degradative processes of polymeric materials (Watts et al., 2003; Shi et al., 2011; Dintcheva et al., 2016a). This intriguing property of CNTs seems to be related mainly to a radical scavenging mechanism (Galano, 2008; Galano et al., 2010); specifically, CNTs, similarly to other carbon-based nanostructures such as graphene and fullerenes, are able to act as radical traps, reacting with the macro-radicals formed during polymer degradation (Martinez-Morlanes et al., 2012; Dintcheva et al., 2015a). The radical scavenging activity of CNTs is related to their acceptor-like electronic properties: due to the presence of lattice defects, CNTs possess acceptor-like localized states which are invoked as the main responsible for the radical termination (Dintcheva et al., 2015b). Furthermore, the UV stabilizing action of CNTs has been attributed to their photo-induced oxidation that occurs when they are exposed simultaneously to UV light and oxygen. Owing to this mechanism, the formation of locally electron-deficient and electron-rich regions onto the CNTs outer surface occurs. In this way, the oxygen molecules are adsorbed onto the formed electron-rich zones and are no longer available for polymer oxidation (Savage et al., 2003; Guadagno et al., 2010).

In recent studies reported in literature, the radical scavenging activity of CNTs has been amplified through the immobilization of molecules carrying anti-oxidant function onto the CNTs outer surface, considering two different approaches: covalent grafting and physical absorption (Arrigo et al., 2015; Dintcheva et al., 2014; Dintcheva et al. 2016b). In particular, natural stabilizing molecules, such as vitamin E and quercetin, have been physically immobilized onto the CNTs outer surface, and the obtained multi-functional fillers significantly improved the thermo-oxidation stability of a host polymeric matrix. Apart from the stabilizing activity of the functional moieties, this result was ascribed to an amplification of the inherent radical scavenging activity of CNTs, due to the strong interactions established between the carbon atoms of the CNTs surface and the immobilized molecules, which promote the formation of CNTs structural defects.

In this work, hybrid nanoparticles consisting of CNTs and a hindered phenol commercial anti-oxidant have been formulated through two different strategies: physical immobilization and covalent grafting. The nano-hybrids have been used as nanofillers in UHMWPE-based nanocomposites, with the dual aim to improve the state of polymer/nanoparticles interface and to enhance the nanocomposites thermo-oxidative stability.

2. Materials and methods

2.1. Materials

The UHMWPE is a commercial grade purchased by Sigma–Aldrich. It has weight-average molecular weight $3 \div 6$ MDa, softening point T = 136°C (Vicat, ASTM D 1525B), melting point T_m = 138 °C (determinate by DSC) and density 0.94 g/mL at 25 °C.

Multiwalled Carbon Nanotubes, CNTs, were prepared by the typical Chemical Vapor Deposition (CVD) protocol, using ethylene as carbon source (Dintcheva et al. 2016a). The purification was performed with 50% aqueous sulfuric acid, obtaining Carbon Nanotubes with outer diameters ranging between 14 and 20 nm, inner diameters in the range of 2–5 nm, length $1 \div 10$ μm, and purity >98 wt%. After the purification process the content of carboxylic groups was estimated to be $0.5 \div 1$% by means of XPS analysis and acid/base titration.

Irganox 1010 (Pentaerythritol Tetrakis(3-(3,5-di-tert-butyl-4-h ydroxyphenyl)propionate)), Irg1010, is a is an ex. Ciba® Specialty Chemicals (BASF).

All chemical reagents have been purchased by Sigma–Aldrich® and used as received.

2.2. CNTs functionalization

The Irg1010-f-CNTs have been obtained through a procedure summarized in Fig. 1. In particular, 350 g of HO-alkyl-f-CNTs, prepared following a procedure reported elsewhere (Dintcheva et al., 2016b), have been dispersed in a solution of Irg1010 (1.0 g) and Potassium tert-butoxide (0.21 g) in 150 ml of DMSO. The resulting mixture was sonicated in a ultrasound bath (240 W, 2.5 Lt) for 3 min, and then it was stirred at 80 °C for 24 h. After that, the suspension was filtered on a sintered glass filter and then the Irg1010-f-CNTs (**2**) were carefully washed with hot methanol, and finally dried at 90 °C overnight.

To prepare Irg1010@CNTs, Irg1010 molecules have been immobilized onto the outer surface of the CNTs as follow (see Fig. 1): 0.4 g of bare CNTs were dispersed in a solution of Irg1010 (0.2 g) in 30 ml of THF. The resulting suspension was sonicated in a 2 L ultrasonic bath (power 260 W) for 30 min to allow for the physical absorption of the anti-oxidant onto the CNTs. Then, the solute was filtered on a sintered glass filter and then the Irg1010@CNTs (**3**)
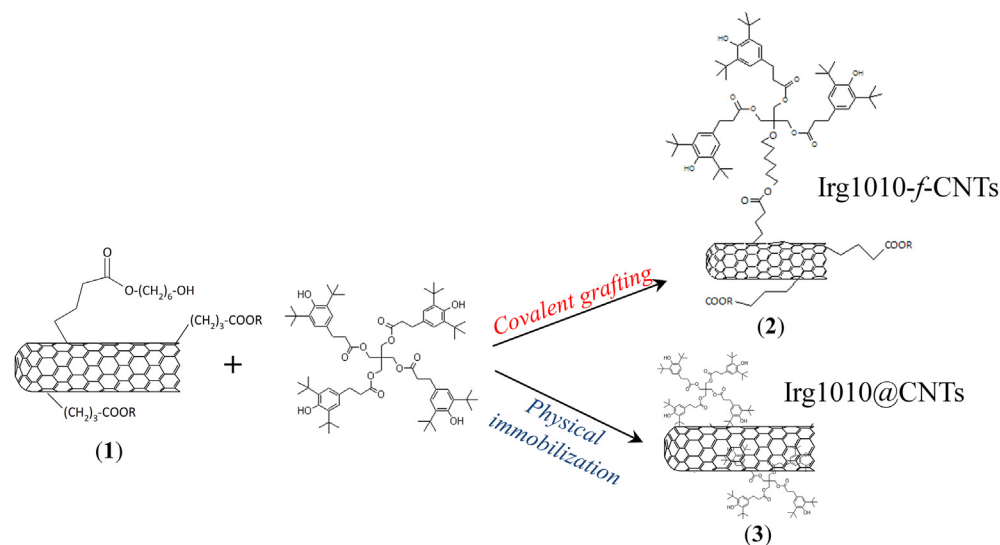

Fig. 1. Synthesis of hybrid nanoparticles.

were carefully washed with THF, and finally dried at 90 °C overnight.

2.3. Nanocomposite preparation

The UHMWPE powder and 1 wt% of CNTs were manually mixed at room temperature until a homogeneous black powder was obtained. Then the blends were hot compacted at 210 °C for 5 min and under a pressure of 1500 psi to get thin films (thickness less than 100 mm) for the subsequent analyses. The pure UHMWPE and UHMWPE/Irg1010 (containing 0.1 wt% of free Irg1010 molecules) films used as reference materials were subjected to the same procedure.

2.4. Characterizations

Micro-Raman spectroscopy has been performed at room temperature through a Renishaw Invia Raman Microscope equipped with a 532 nm Nd:YAG laser excitation and 100 mW power. Non-confocal measurements were carried out in the range 3200–100 cm^{-1} with a spectral resolution between 0.5 and 1 cm^{-1}.

Applied Biosystems 4800 MALDI TOF/TOF TM Analyzer (Framingham, MA) mass spectrometer was used in this study to acquire MALDI spectra. The TOF/TOF instrument is equipped with a Nd: YAG laser (355 nm wavelength) of <500 ps pulse and 200 Hz repetition rate. MALDI-TOF/TOF-MS spectra were recorded in reflector positive ion mode. The MALDI analyses were performed following the procedure reported elsewhere (Carroccio et al., 2013).

ATR-FTIR analysis was performed using a Fourier Transform Infrared Spectrometer (FTIR) (Spectrum Two FTIR spectrometer, Perkin Elmer) equipped with a diamond crystal for surface analysis. Spectra collected on three different batches of each sample (milligramme level) were obtained by accumulation of 32 scans between 4000 and 400 cm^{-1}, with a resolution of 4 cm^{-1}.

Thermo-Gravimetric analysis (TGA) was carried out using an Exstar TG/DTA Seiko 7200 instrument with a heating rate of 10 °C/min from 30 to 700 °C under nitrogen flow. The reported results are the average of three independent measurements on batches (around 5 mg) of CNTs. The standard deviation was about 0.4% for each investigated sample.

Rheological tests were performed using a strain-controlled rotational rheometer (ARES G2 by TA Instruments) in parallel plate geometry (plate diameter 25 mm). The complex viscosity (η^*) was measured performing frequency sweep tests at T = 210 °C from 10^{-2} to 10^2 rad/s at a maximum strain of 2%. As proved by preliminary strain sweep experiments, such an amplitude is low enough to be in the linear viscoelastic regime. Besides, linear stress relaxation measurements were carried out submitting the samples to a single step strain $\gamma_0 = 1\%$, and the shear stress evolution during time $\sigma(t)$ was measured to obtain the relaxation modulus G(t) = σ(t)/γ_0.

Optical microscopy was performed using a Leica Microscope in reflection mode at a magnification of 20X. Images were acquired on the surface of the nanocomposite films.

Crystallization behaviour of neat UHMWPE and formulated nanocomposites has been investigated by Differential scanning calorimetry (DSC), using a Perkin-Elmer DSC7 calorimeter. All experiments were performed under dry N$_2$ gas using samples of around 10 mg in 40 μL sealed aluminium pans. Four calorimetric scans (two heating: 30–180 °C and two cooling: 180–30 °C) were performed for each sample at scanning heating/cooling rate of 10 °C/min.

The crystallinity degree (X$_c$) is calculated using the formula:

$$X_c(\%) = \frac{\Delta H_m}{\Delta H^0 (1 - W_f)}$$

where ΔH_m is the heat of melt of sample, $\Delta H°$ is the heat of fusion for 100% crystalline UHMWPE (289 J/g) (Arrigo et al., 2016a) and W$_f$ the mass fraction of the nanofiller. The reported results are the average of three independent measurements.

A Fourier Transform Infrared Spectrometer (FTIR) (Spectrum Two FTIR spectrometer, Perkin Elmer) was used to record the infrared spectra. FT-IR analyses were carried out to infer the advance of the degradation phenomena on nanocomposite films.

Specifically, the samples were first treated in an air oven at T = 120 °C, which is a temperature lower than the T$_m$ of the polymer but high enough to accelerate the degradation processes. Then, FT-IR spectra were collected performing 16 scans between 4000 and 500 cm^{-1} on samples subjected to thermo-oxidation for different exposure times. The carbonyl index (CI) was calculated as the ratio between the carbonyl absorption area (1850–1600 cm^{-1}) and the area of a reference peak at about 2019 cm^{-1}. Since this index is strictly related to the degradation phenomena, the progress of the latter was followed by monitoring the evolutions of CI with the thermo-oxidation time.

3. Results and discussion

3.1. Assessment of the CNTs functionalization

In order to verify the success of the CNTs functionalization procedure, MALDI-TOF MS analysis has been carried out. Since Irg1010-*f*-CNTs cannot be directly used as MALDI analyte because of their high molecular weight, the functionalized nanoparticles were subjected to a thermal cleavage before the MALDI measurements. As a result, the CNTs and the functionalizing groups obtained after hydrolysis of Irg1010-*f*-CNTs represent the matrix and analyte, respectively. This approach allows for the univocal identification of the functionalizing group anchored to the CNTs surface and the demonstration of the covalent linkage. The collected MALDI MS spectrum, reported in Fig. 2(a), shows a series of signals at m/z 853.09 and 869.05, attributable to some clusters coming from the matrix or to impurities introduced during the functionalization procedure, and two intense peaks at m/z 1059.22 and 1075.20 which can be ascribed to the structures (1) and (2) depicted in Fig. 2(a), respectively desorbing as protonated ions. The absence of any noticeable peak related to the presence of the Irg1010 molecules excludes the presence of Irg1010 molecules adsorbed onto the CNTs surface and confirms the structure of Irg1010-*f*-CNTs hybrid nanoparticles proposed in Fig. 1.

Additional proofs about the obtainment of the nano-hybrids come from Raman analysis, see spectra of bare CNTs and Irg1010-*f*-CNTs reported in Fig. 2(b). For comparison, in the same Figure the Raman spectrum of the HO-alkyl-*f*-CNTs is reported. Two prominent peaks can be noticed at about 1340 and 1375 cm^{-1}; the first, known as defect-induced disorder mode (D band), is related to the carbon atoms containing structural defects, while the second is identified as the tangential mode (G band) and refers to the in-plane vibrational motion of the carbon atoms (Castell et al., 2013). Usually, the ratio I$_D$/I$_G$ between the intensities of the two aforementioned bands is used to qualitatively estimate the content of structural defects in CNTs (Jung et al., 2012). In the case of bare CNTs, the values of the I$_D$/I$_G$ ratio is about 0.48, while it significantly increases for functionalized CNTs; particularly, for HO-alkyl-*f*-CNTs and Irg1010-*f*-CNTs, the values of I$_D$/I$_G$ ratio are 1.15 and 1.25, respectively. This feature suggests the damage of the CNTs outer surface due to the covalent functionalization. It is worth nothing that the I$_D$/I$_G$ ratio of Irg1010-*f*-CNTs sample is slightly higher than that of HO-alkyl-*f*-CNTs sample, probably due to the further damage of CNTs outer surface induced by ultra-sound treatment during the second step of functionalization
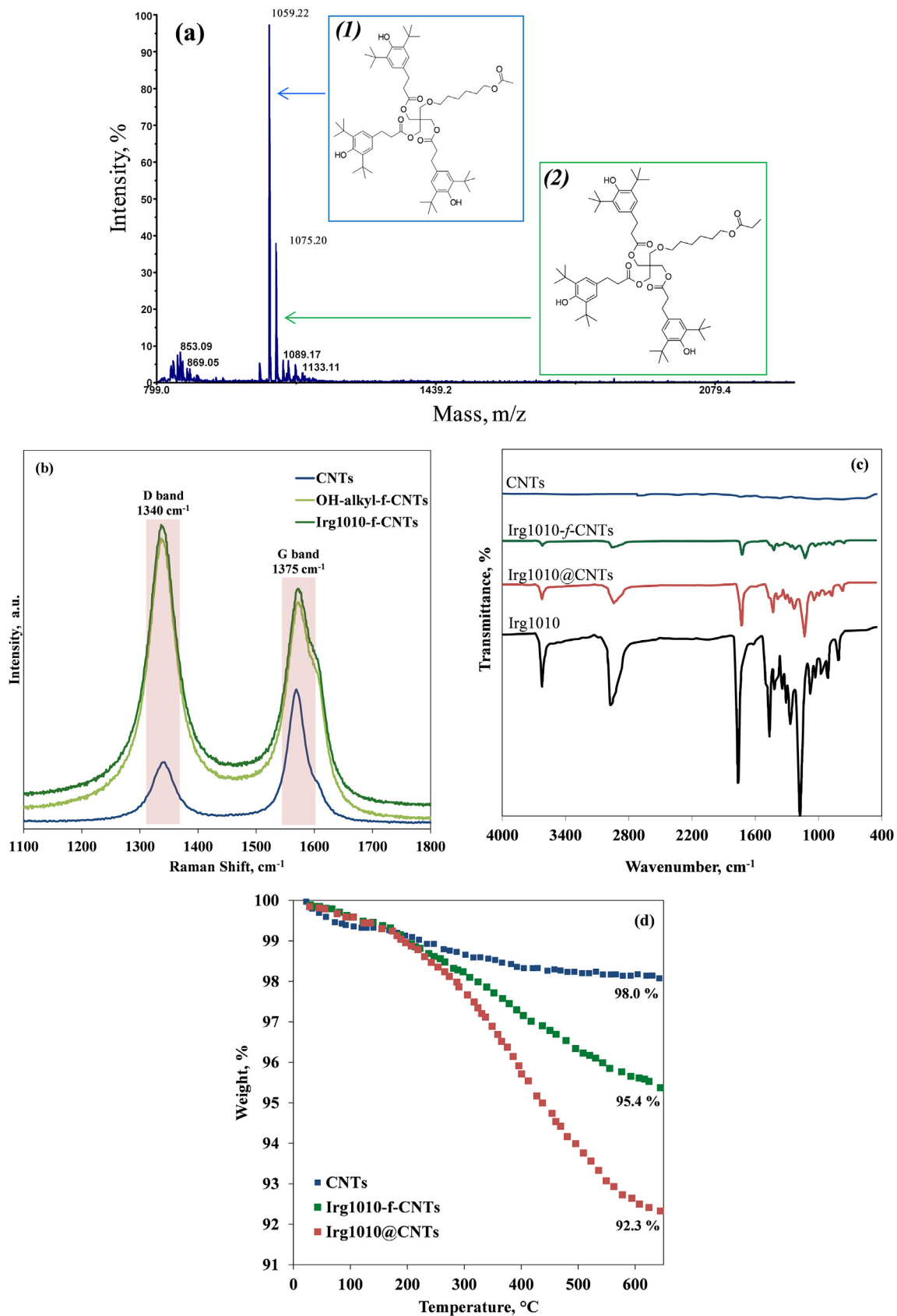
Fig. 2. MALDI-TOF MS spectrum registered in reflection and positive mode (a), Raman spectra (b), ATR-FTIR spectra (c) and TGA curves (d) of bare CNTs, functionalized CNTs and nano-hybrids.

process. The successful of the functionalization procedure is also confirmed by the appearance of a shoulder at about 1610 cm^{-1} in the Raman spectrum of the functionalized CNTs, which can be associated with carbon atoms from the grafted molecules which, having sp^3 hybridization, interfere with the CNTs aromatic system (Lonkar et al., 2012).

The presence of Irg1010 molecules onto the CNTs surface has been investigated through ATR-FTIR analyses, see spectra reported in Fig. 2 (c). The ATR-FTIR spectrum of pure Irg1010 molecules shows the characteristic bands corresponding to: (*i*) phenolic groups absorption band (3600 cm^{-1}); (*ii*) carbonyl ester groups (1740 cm^{-1}); (*iii*) symmetric (1040 cm^{-1}) and asymmetric (1275 cm^{-1}) stretching of C-O-C groups; (*iv*) symmetric (765 cm-^{1}) and asymmetric (1140 cm^{-1}) C–H bending (Barbeş et al., 2014). Such specific bands are clearly detectable in the spectra of both Irg1010-*f*-CNTs and Irg1010@CNTs, revealing the presence of Irg1010 molecules in these samples. More convincing proofs about the presence of Irg1010 molecules onto the surface of functionalized CNTs come from the results of thermogravimetric analyses reported in Fig. 2(d). Both hybrid nanoparticles decompose at temperature lower than bare CNTs, because of the volatilization of the Irg1010 molecules grafted or physically immobilized on the CNTs surface. The residues at the end of the analysis was 95.4 and 92.3% for Irg1010-*f*-CNTs and Irg1010@CNTs, respectively, while a residue of 98.0% was found for the bare CNTs. The relative amount of Irg1010 onto CNTs can be estimated by the TGA analysis. The difference in weight at 600 °C between hybrid nanoparticles and bare CNTs showed that the content of immobilized Irg 1010 is about 2.6 wt% in Irg1010-*f*-CNTs and 5.7 wt% in Irg1010@CNTs. It is worth noting that the gradual weight loss related to the thermal decomposition of the Irg1010 groups takes place in the range 300 to 500 °C, i.e. well above the temperature at which the nanocomposite thin films were prepared and characterized.

3.2. Characterization of UHMWPE-based nanocomposites

Rheological analyses can provide useful information in terms of state of dispersion of nanoparticles in polymer-based nanocomposites, since if the nanofillers are homogeneously dispersed in the host matrix, they are able to affect the polymer relaxation spectrum. Moreover, the results coming from rheological measurements can be profitably used to investigate the state of the polymer/nanofillers interface in multi-phase polymer nanocomposites. The complex viscosity (η*) and storage modulus (G') of neat UHMWPE and all formulated nanocomposites are shown in Fig. 3 as a function of frequency. At low frequencies, neat UHMWPE exhibit the typical Newtonian plateau, due to the fully relaxed macromolecules; as the frequency increases, a pronounced shear thinning behaviour, due to the alignment of the UHMWPE chains with the flow, can be noticed. It is clear from viscosity trends reported in Fig. 3(a) that the adding of all kinds of CNTs affects the rheological behaviour of the host matrix. First of all, the η* values of the nanocomposites are higher than those of neat UHMWPE, particularly at low frequency, where the melt state dynamics of large portion of macromolecules are probed. Moreover, the disappearance of the Newtonian plateau, especially for the nanocomposites containing the nano-hybrids, suggests the arrangement of the functionalized CNTs in interconnected structures with the formation of a percolative network of nanoparticles into the host matrix. Fig. 3(b) shows the trends of the storage modulus as a function of frequency for all investigated systems. At low frequencies, neat UHMWPE exhibits typical homopolymer-like terminal behaviour, with the scaling properties of G' ≈ ω^2, see the values reported in the inset. The adding of all kinds of CNTs leads to an increase of the G' values in the whole investigated frequency range
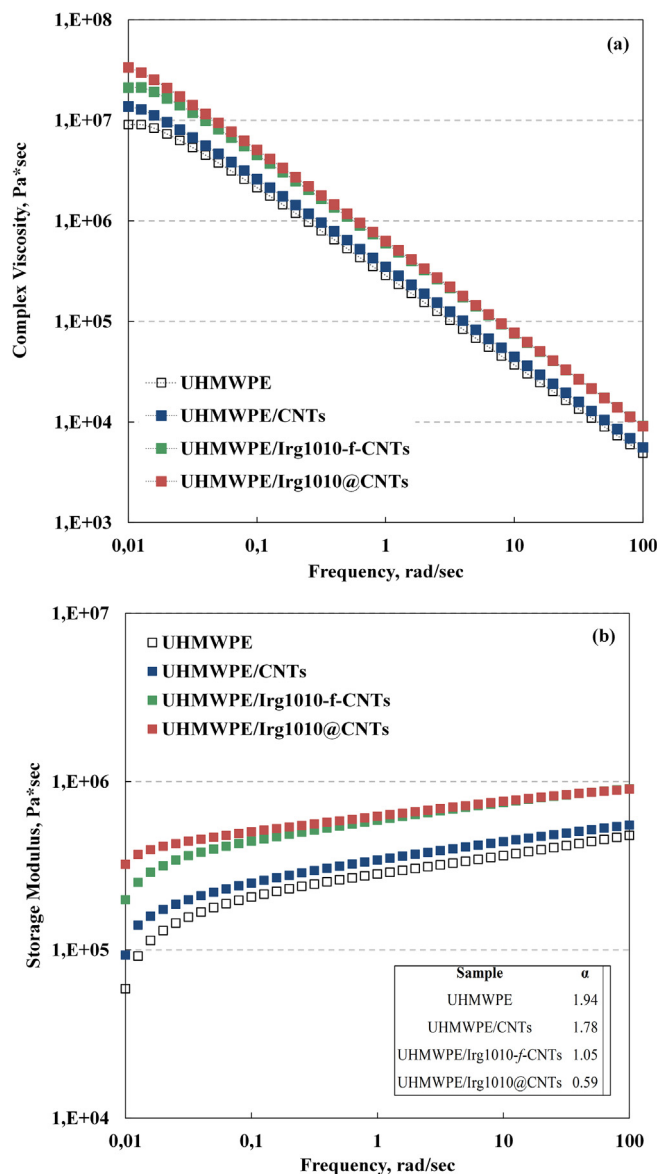

Fig. 3. Complex viscosity (a) and Storage Modulus (b) for UHMWPE-based nanocomposites. The rheological functions of neat UHMWPE are reported for comparison.

and this effect is consistent with the addition of solid particles into a polymer matrix. Furthermore, as a consequence of the nanoparticles addition, the terminal behavior tends to disappear and the modulus G' of the nanocomposites containing the nano-hybrids tends to become frequency-independent. Indeed, the slope of G' vs frequency, evaluated at low frequency, decreases from about 1.8 for the UHMWPE/CNTs nanocomposite to 1.0 and 0.6 for UHMWPE/Irg1010-*f*-CNTs and UHMWPE/Irg1010@CNTs, respectively. This non-terminal low frequency behavior indicates the occurrence of a transition from liquid-like to solid-like rheological behavior and can be attributed to the formed CNTs network, which restrains the long-range motion of polymer chains. The ability of dispersed CNTs to hinder the relaxation of UHMWPE macromolecular chains has been confirmed by transient stress relaxation measurement, performed at low strain in order to assure linear regime, see the results reported in Fig. 4. It can be observed that, for any fixed time after the imposition of strain, the modulus G(t) increases with the adding of both unmodified and functionalized CNTs and, similarly to that observed in the dynamic
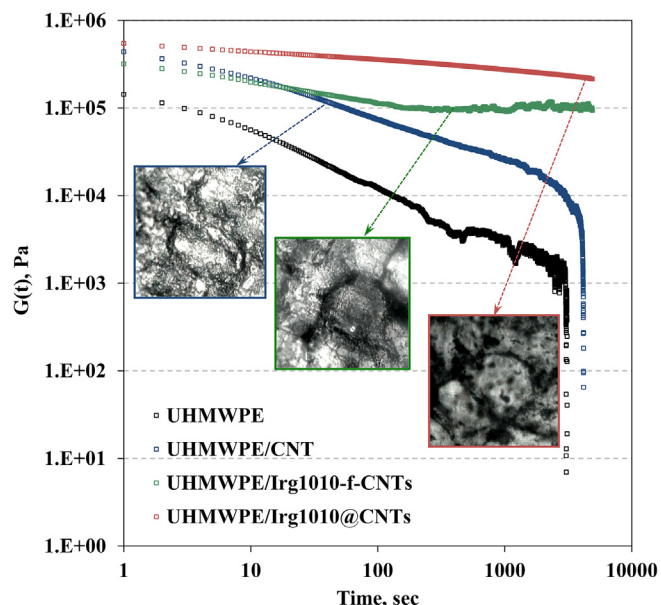
Fig. 4. Stress relaxation modulus for neat UHMWPE and all investigated nanocomposites.

Fig. 5. Thermograms recorded during the second heating scan for neat UHMWPE and UHMWPE-based nanocomposites.

viscoelastic measurements, the enhancement of G(t) is more pronounced for the hybrid nanoparticles having immobilized Irg1010 molecules. Furthermore, while at short times the stress relaxation behavior is qualitatively similar for the nanocomposites and for the unfilled polymer, at long times the neat matrix and the nanocomposites show different relaxation kinetics. In particular, neat UHMWPE and UHMWPE/CNTs nanocomposite relax like a liquid, although the unfilled matrix relaxes quickly than the CNTs-containing nanocomposite, in which the macromolecules, due to the CNTs presence, employ longer times to recover their relaxed configuration after the imposing of the strain. On the contrary, the adding of both Irg1010-*f*-CNTs and Irg1010@CNTs significantly modify the long-time relaxation and the nanocomposites behave like a pseudo-solid material; indeed the stress relaxes to an equilibrium value rather than relaxing to zero and this behaviour probably occurs due to the formation of a three-dimensional superstructure of nano-hybrids within the host UHMWPE. The alterations of the polymer rheological behavior noticed upon the CNTs adding are more pronounced in presence of the nano-hybrids. This issue can be likely attributed to the beneficial effect of the immobilized Irg1010 molecules that, being gathered at the polymer/nanoparticles interface, enhance the interfacial binding between the two phases, leading to an improvement of the state of the interfacial region.

In Fig. 4, representative optical micrographs of UHMWPE-based nanocomposites are reported. As a result of the method used for the nanocomposites formulation, a segregated morphology has been obtained, with the preferential localization of CNTs in the interfacial region and the formation of CNTs-rich channels surrounding UHMWPE-rich islands. Comparison between the morphology of bare CNTs and nanohybrids-based nanocomposites indicates that in the former a broader segregated networks within host matrix has been obtained. The presence of Irg1010 molecules immobilized onto the CNTs surface in nano-hybrids-based nanocomposites, avoid the CNTs agglomeration and allows the formation of a well-ordered segregated structure.

To assess the influence of CNTs adding on the crystallization behaviour of UHMWPE, DSC analyses have been performed. In Fig. 5 the thermograms recorded during the second heating scan for neat UHMWPE and CNTs-containing nanocomposites are
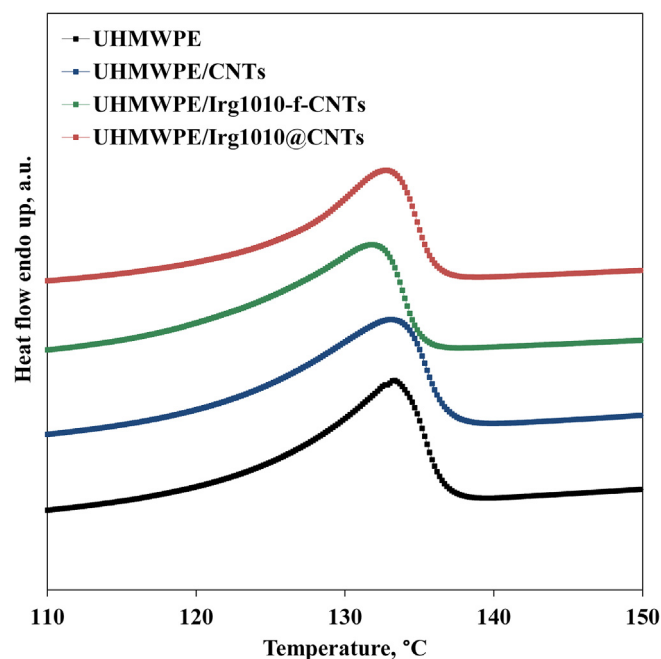
reported. Moreover, in Table 1 the relevant data, such as melting temperature, melting enthalpy and crystallinity degree, are listed. It can be observed that the adding of bare and functionalized CNTs has a negligible effect on the melting temperature while leads to a decrease of the crystallinity degree with respect to the neat matrix, that is more pronounced in presence of nano-hybrids. This issue can be explained considering that the dispersed CNTs disturb the crystallization process of UHMWPE chains and this feature is exacerbated in presence of functionalized CNTs, as the steric hindrance of the Irg1010 molecules immobilized on the CNTs surface hampers the crystallization process of UHMWPE macromolecules close to the CNTs surface.

3.3. Thermo-oxidative behaviour of UHMWPE-based nanocomposites

The thermo-oxidation behaviour of neat UHMWPE and UHMWPE-based nanocomposites has beeninvestigated through the analysis of the evolution in time of the FT-IR spectra of the neat matrix and nanocomposites, collected at regular time intervals during a thermo-oxidation treatment performed in an air oven at 120 °C. In particular, the carbonyl index (CI) shown in Fig. 6 has been used to monitor the progress of the oxidative processes. The CI is related to the intensity of the intensity bands in the range 1850–1600 cm^{-1} (see inset in Fig. 6), arising from the formation of carboxylic acids (1713 cm^{-1}), ketones (1718 cm^{-1}), esters (1738 cm^{-1}), lactones (1786 cm^{-1}), and other oxygen-containing species coming from UHMWPE oxidative degradation (Costa et al., 1997). Concerning the thermo-oxidative behaviour of neat

Table 1
Calorimetric data for neat UHMWPE and all investigated UHMWPE-based nanocomposites.

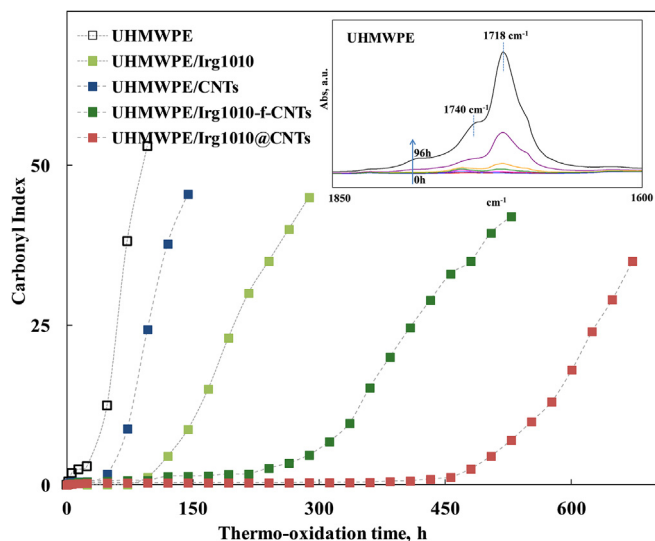| Sample	T$_{melt}$, °C	ΔH$_{melt}$, J/g	Crystallinity Degree, %
UHMWPE	133.4	139.7	48.0
UHMWPE/CNTs	133.0	134.2	46.9
UHMWPE/Irg1010-*f*-CNTs	131.7	123.3	43.0
UHMWPE/Irg1010@CNTs	132.7	118.1	41.2

Fig. 6. Carbonyl Index as a function of the thermo-oxidation time for neat UHMWPE, UHMWPE/Irg1010 system and UHMWPE-based nanocomposites.

UHMWPE, the build-up curve of CI increases suddenly, suggesting that the degradation of neat matrix begins at the early stage of the oxidative treatment. The nanocomposite containing bare CNTs shows a more pronounced thermo-oxidative resistance with respect to neat matrix, due to the well-known radical scavenging activity of CNTs. The addition of both kinds of hybrid nanoparticles brings about the obtainment of a remarkable enhanced thermo-oxidative stability with respect to the neat matrix and to the nanocomposite containing bare CNTs. Indeed, a dramatic improvement of the induction time can be noticed for the nanocomposites containing both Irg1010-f-CNTs and Irg1010@CNTs nanohybrids. Additionally both nanocomposites exhibit a slower growth rate of CI after the induction period. Therefore, the nano-hybrids are able to exert a remarkable anti-oxidant activity that is significantly higher than what one would expect considering the effect of CNTs and Irg1010 molecules added one by one. Indeed, as shown in Fig. 6, even adding 0.1 wt% of Irg1010 free molecules (i.e. not immobilized), that is to say an amount of antioxidant much higher than that actually present in our nanocomposite samples, the improvement of the thermo-oxidation resistance is much less important.

To explain the obtained results it can be argued that, in a similar way to what probed in the case of CNTs bearing immobilized naturally occurring anti-oxidant molecules, such as α-tocopherol and quercetin (Dintcheva et al., 2014; Arrigo et al., 2015), the presence of Irg1010 molecules close to the CNTs surface can induce the formation of CNTs structural defects and amplify the CNTs radical scavenging activity. In more detail, due to the strong interactions established between the Irg1010 molecules and CNTs, some carbon atoms on the CNTs outer surface change the hybridization from sp^2 to sp^3, inducing the formation of structural defects which, in turn, results in the formation of acceptor-like localized states inducing an amplified radical scavenging activity of CNTs. Furthermore, being immobilized onto CNTs outer surface, Irg1010 molecules are able to exert their anti-oxidant action in the interfacial region between polymer chains and nanoparticles, that represent the critical zone for the trigger of the degradation phenomena.

4. Conclusions

Anti-oxidant Irg1010 molecules have been immobilized onto the surface of CNTs following two different approaches, i.e. covalent anchoring and physical absorption, and the so obtained

nano-hybrids have been dispersed in UHMWPE with the dual aim to improve the state of the polymer/nanoparticle interface and enhance the thermo-oxidative stability of nanocomposites. The evaluation of the rheological behavior of UHMWPE-based nanocomposites indicates that the immobilization of the Irg1010 molecules is beneficial to obtain a more homogeneous dispersion of functionalized CNTs within the host polymer matrix. furthermore, the monitoring of the thermo-oxidative processes trough FTIR analysis shows that the nano-hybrids offer a remarkable stabilizing activity which is related to the synergic effect stemming from the strong interactions between Irg1010 molecules and CNTs.

Funding

References

Arrigo, R., Dintcheva, N.T., Guenzi, M., Gambarotti, C., Filippone, G., Coiai, S., Carroccio, S., 2015. Thermo-oxidative resistant nanocomposites containing novel hybrid-nanoparticles based on natural polyphenol and carbon nanotubes. Polym. Degrad. Stab. 115, 129–137.

Arrigo, R., Dintcheva, N.T., Pampalone, V., Morici, E., Guenzi, M., Gambarotti, C., 2016a. Advanced nano-hybrids for thermo-oxidative-resistant nanocomposites. J. Mater. Sci. 51, 6955–6966.

Arrigo, R., Dintcheva, N.T., Guenzi, M., Gambarotti, C., 2016b. Nano-hybrids based on quercetin and carbon nanotubes with excellent anti-oxidant activity. Mater. Lett. 180, 7–10.

Barbeş, L., Rădulescu, C., Stihi, C., 2014. ATR-FTIR spectrometry characterisation of polymeric materials. Romanian Rep. Phys. 66, 765–777.

Carroccio, S.C., Curcuruto, G., Dintcheva, N.T., Gambarotti, C., Coiai, S., Filippone, G., 2013. Using matrix-assisted laser desorption/ionization time-of-flight mass spectrometry for the characterization of functionalized carbon nanotubes. Rapid Commun. Mass Spectrom. 27, 1359–1366.

Castell, P., Martinez-Morlanes, M.J., Alonso, P.J., Martinez, M.T., Puertolas, J.A., 2013. A novel approach to the chemical stabilization of gamma irradiated ultrahigh molecular weight polyethylene using arc-discharge multi-walled carbon nanotubes. J. Mater. Sci. 48, 6549–6557.

Chen, W., Duan, L., Wang, L., Zhu, D., 2008. Adsorption of hydroxyl- and amino-substituted aromatics to carbon nanotubes. Environ. Sci. Technol. 42, 6862–6868.

Coleman, J.N., Khan, U., Blau, W.J., Gun'ko, Y.K., 2006. Small but strong: a review of the mechanical properties of carbon nanotube-polymer composites. Carbon 44, 1624–1652.

Costa, L., Luda, M.P., Trossarelli, L., 1997. Ultra high molecular weight polyethylene – II. Thermal- and photo-oxidation. Polym. Degrad. Stab. 58, 41–54.

Dintcheva, N.T., Arrigo, R., Gambarotti, C., Carroccio, S., Filippone, G., Cicogna, F., Guenzi, M., 2014. α-Tocopherol-induced radical scavenging activity in carbon nanotubes for thermo-oxidation resistant ultra-high molecular weight polyethylene-based nanocomposites. Carbon 74, 14–21.

Dintcheva, N.T., Arrigo, R., Gambarotti, C., Carroccio, S., Coiai, S., Filippone, G., 2015a. Advanced ultra-high molecular weight polyethylene/antioxidant-functionalized carbon nanotubes nanocomposites with improved thermo-oxidative resistance. J. Appl. Polym. Sci. 132, 42420.

Dintcheva, N.T., Arrigo, R., Morici, E., Gambarotti, C., Carroccio, S., Cicogna, F., Filippone, G., 2015b. Multi-functional hindered amine light stabilizers-functionalized carbon nanotubes for advanced ultra-high molecular weight Polyethylene-based nanocomposites. Compos. Part B Eng. 82, 196–204.

Dintcheva, N.T., Arrigo, R., Teresi, R., Megna, B., Gambarotti, C., Marullo, S., D'Anna, F., 2016a. Tunable radical scavenging activity of carbon nanotubes through sonication. Carbon 107, 240–247.

Dintcheva, N.T., Arrigo, R., Carroccio, S., Curcuruto, G., Guenzi, M., Gambarotti, C., Filippone, G., 2016b. Multi-functional polyhedral oligomeric silsesquioxane-functionalized carbon nanotubes for photo-oxidative stable Ultra-High Molecular Weight Polyethylene-based nanocomposites. Eur. Polym. J. 75, 525–537.

Galano, A., 2008. Carbon nanotubes as free-radical scavengers. J. Phys. Chem. C 112, 8922–8927.

Galano, A., Francisco-Marquez, M., Martínez, A., 2010. Influence of point defects on the free-radical scavenging capability of single-walled carbon nanotubes. J. Phys. Chem. C 114, 8302–8308.

Guadagno, L., Naddeo, C., Raimondo, M., Gorrasi, G., Vittoria, V., 2010. Effect of carbon nanotubes on the photo-oxidative durability of syndiotactic polypropylene. Polym. Degrad. Stab. 95, 1614–1626.

Jie, G., Kongyin, Z., Xinxin, Z., Zhijiang, C., Min, C., Tian, C., Junfu, W., 2015. Preparation and characterization of carboxyl multi-walled carbon nanotubes/calcium alginate composite hydrogel nano-filtration membrane. Mater. Lett. 157, 112–115.

Jung, W.R., Choi, J.H., Lee, N., Shin, K., Moon, J.H., Seo, Y.S., 2012. Reduced damage to carbon nanotubes during ultrasound-assisted dispersion as a result of supercritical-fluid treatment. Carbon 50, 633–636.

Lin, D., Xing, B., 2008. Adsorption of phenolic compounds by carbon nanotubes: role of aromaticity and substitution of hydroxyl groups. Environ. Sci. Technol. 42, 7254–7259.

Lonkar, S.P., Kushwaha, O.S., Leuteritz, A., Heinrich, G., Singh, R.P., 2012. Self photostabilizing UV-durable MWCNT/polymer nanocomposites. RSC Adv. 2, 12255–12262.

Mallakpour, S., Soltanian, S., 2016. Efficient surface modification of MWCNTs with vitamin B1 and production of poly(ester-imide), MWCNTs nanocomposites containing L-phenylalanine moiety: thermal and microscopic study. Express Polym. Lett. 10, 54–64.

Martinez-Morlanes, M.J., Castell, P., Alonso, P.J., Martinez, M.T., Puertolas, J.A., 2012. Multiwalled carbon nanotubes acting as free radical scavengers in gamma-irradiated ultrahigh molecular weight polyethylene composites. Carbon 50, 2442–2452.

Mawhinney, D.B., Naumenko, V., Kuznetsova, A., Yates, J.T., Liu, J., Smalley, R.E., 2000. Surface defect site density on single walled carbon nanotubes by titration. Chem. Phys. Lett. 324, 213.

Nativ-Roth, E., Shvartzman-Cohen, R., Bounioux, C., Florent, M., Zhang, D., Szleifer, I., Yerushalmi-Rozenet, R., 2007. Physical adsorption of block copolymers to SWNT and MWNT: a nonwrapping mechanism. Macromolecules 40, 3676–3685.

Pan, B., Xing, B., 2008. Adsorption mechanisms of organic chemicals on carbon nanotubes. Environ. Sci. Technol. 42, 9005–9013.

Savage, T., Bhattacharya, S., Sadanadan, B., Gaillard, J., Tritt, T.M., Sun, Y.-P., Wu, Y., Nayak, S., Car, R., Marzari, N., Ajayan, P.M., Rao, a.M., 2003. Photoinduced oxidation of carbon nanotubes. J. Phys. Condens. Matter 15, 5915–5921.

Shi, X., Jiang, B., Wang, J., Yang, Y., 2011. Influence of wall number and surface functionalization of carbon nanotubes on their antioxidant behavior in high density polyethylene. Carbon 50, 1005–1013.

Spitalsky, Z., Tasis, D., Papagelis, K., Galiotis, C., 2010. Carbon nanotube–polymer composites: chemistry, processing, mechanical and electrical properties. Prog. Polym. Sci. 35, 357–401.

Wang, X., Liu, Y., Tao, S., Xing, B., 2010. Relative importance of multiple mechanisms in sorption of organic compounds by multiwalled carbon nanotubes. Carbon 48, 3721–3728.

Watts, P.C.P., Fearon, P.K., Hsu, W.K., Billingham, N.C., Kroto, H.W., Walton, D.R.M., 2003. Carbon nanotubes as polymer antioxidants. J. Mater. Chem. 13, 491–495.

Yang, M., Gao, Y., Li, H., Adronov, A., 2007. Functionalization of multiwalled carbon nanotubes with polyamide 6 by anionic ring-opening polymerization. Carbon 45, 2327–2333.

Yu, S., Wang, X., Ai, Y., Tan, X., Hayat, T., Hu, W., Wang, X., 2016. Experimental and theoretical studies on competitive adsorption of aromatic compounds on reduced graphene oxides. J. Mater. Chem. A 4, 5654–5662.